

Electron Cloud Instabilities in the Damping Ring of International Linear Collider

K. Ohmi

KEK, Oho, Tsukuba, Ibaraki, 305-0801, Japan

Damping rings of Linear Collider are very low emittance ($\varepsilon < 1\text{nm}$) storage rings which accumulate many electron and positron bunches during several damping times. The positron damping ring seems to be serious for electron cloud instability obviously. We discuss electron cloud instability for the damping ring of International Linear Collider (ILC).

1. INTRODUCTION

We discuss electron cloud effects in ILC positron damping ring. The positron damping ring stores positron beam during several damping time and extracts very low emittance beam to the main linac. The damping ring accumulates 2800 positron bunches of the population of 2×10^{10} in the circumference. There are several choices for the circumference and lattice design. They are listed in Table 1. The positron beam emits synchrotron radiation photons, which create a large number of photoelectrons at the chamber surface. Though ante-chambers are used to avoid the photoelectrons, considerable rate of photoelectrons and secondary electrons remain in the chamber. Study of the electron cloud effect in the damping ring is one of the most important subjects to realize the linear collider.

Table I: Basic parameters of the ILC damping ring

Lattice		TESLA	MCH	DAS	2xOCS	OCS	BRU	OTW	PPA
circumference	$L(\text{m})$	17,000	15,935	17,014	6,114	6,114	6,333.5	3,223	2,824
energy	E	5.0	5.0	5.0	5.0	5.0	3.74	5.0	5.0
bunch population	N_+	2×10^{10}							
emittance	$\varepsilon_x(\text{nm})$	0.50	0.67	0.61	0.56	0.56	0.38	0.39	0.43
	$\varepsilon_y(\text{nm})$	0.001							
typical beta function	$\beta(\text{m})$	30							
bunch length	$\sigma_z(\text{mm})$	6	9	6	6	6	9	6	6
rms energy spread	$\sigma_E/E(10^{-3})$	1.29	1.30	1.30	1.29	1.29	0.973	1.36	1.27
synchrotron tune	ν_s	0.071	0.15	0.067	0.034	0.034	0.12	0.0418	0.0269
bunch train length	n_{bunch}	2820	18	2820	47	47	36	2559	2350
bunch spacing	$\ell_b(\text{ns})$	20.1	20.0	15.38	6.2	6.2	6.2	4.2	4.0
gap between trains	$\ell_{\text{gap}}(\text{ns})$	0	4	0	8.25	8.25	8	0	0
number of bunch train	n_{tr}	1	157	1	60	60	78	1	1

We discuss single bunch instability, incoherent emittance growth, and coupled bunch instability caused by the electron cloud in Sec.2, 3 and 4, respectively.

2. SINGLE BUNCH INSTABILITY

2.1. analytic approach

A single bunch instability is caused by a short range transverse wake field induced by the electron cloud [1]. The short range wake field is analytically estimated by a simple model: that is, beam and electron cloud with the same transverse size interact with each other. We focus on the vertical instability in this paper. The wake field is represented by a resonator model. The resonator frequency (ω_e) corresponds to oscillation frequency of electrons in the beam field,

$$\omega_{e,y} = \sqrt{\frac{\lambda_+ r_e c^2}{\sigma_y(\sigma_x + \sigma_y)}}, \quad (1)$$

where λ_+ and $\sigma_{x(y)}$ are the beam line density in a bunch and transverse beam sizes, respectively. r_e and c are the electron classical radius and the speed of light, respectively.

The wake field is expressed by

$$W_1(z)[\text{m}^{-2}] = c \frac{R_S}{Q} \exp\left(\frac{\omega_e z}{2Qc}\right) \sin\left(\frac{\omega_e}{c} z\right), \quad (2)$$

where

$$c \frac{R_S}{Q} = K \frac{\lambda_e}{\lambda_+} \frac{L}{\sigma_y(\sigma_x + \sigma_y)} \frac{\omega_e}{c}. \quad (3)$$

The density of electron cloud λ_e , which is local line density near the beam, is related to the electron volume density ρ_e via $\lambda_e = 2\pi\rho_e\sigma_x\sigma_y$. K is enhancement factor due to the cloud size. The wake force can be calculated by a numerical method [1]. K is 2-3 for a sufficient large cloud compare than the beam size. Q characterizes damping of electron coherent motion due to the nonlinear interaction with the beam. Q can be also estimated to be 5-10 for a coasting beam by the numerical method. Q is reduced by other sources which induce a frequency spread of ω_e , namely variations of beam charge density along z and of beam size along s , therefore it is not easy to know the accurate value.

The electron phase advance in the bunch, $\omega_e\sigma_z/c$, is an important parameter for the instability characteristics. A large phase advance helps Landau damping, while it induces a strong cloud piling up and pinching near the beam, with the result that K increases. The wake force with a range characterized by Q is efficient only for a bunch with length, $\omega\sigma_z/c > Q$: that is, the effective Q value is the minimum of true Q value and $\omega\sigma_z/c$.

Keil-Schnell-Boussard criteria for the transverse wake force, which is based on coasting beam model, gives the threshold of the fast head-tail instability. The threshold cloud density for given bunch intensity is expressed by

$$\rho_{e,th} = \frac{2\gamma\nu_s\omega_{e,y}\sigma_z/c}{\sqrt{3}KQr_e\beta L}. \quad (4)$$

where β and ν_s are average vertical beta function and synchrotron tune, respectively. For finite chromaticity (ξ), ω_e is replaced by $\omega_e + \omega_0\xi/\eta$.

The threshold value of electron cloud density is estimated by Eq.(4) for the various type of the damping rings. The results for zero chromaticity are shown in Table 2. The threshold density is given for $K \times Q = 3 \times 5 = 15$ and $\beta = 30$ m, except one case.

2.2. Numerical simulation

Though the wake field approximated by the resonator model permits us to study the instability with the simple analytic formula, the estimation of the threshold includes somewhat ambiguous factors: i.e., for example, how to

Table II: Analytical estimates for fast head-tail instability in ILC damping rings. The enhancement factor is chosen to be $KQ = 15$.

Lattice	TESLA	TESLA ^a	MCH	DAS	OCS	BRU	OTW	PPA	KEKB	PEP-II
$\omega_e\sigma_z/c$	14.5	17.3	15.9	13.3	12.6	17.5	14.7	15.4	3.1	
$\rho_{e,th}(10^{12} \text{ m}^{-3})$	0.54	1.29	1.34	0.47	0.62	2.28	1.70	1.31	0.53	

$${}^a\beta = 15 \text{ m}$$

choose K and Q . Since K is related to pinching, one may choose $K \sim \omega_e\sigma_z/c$. A value of Q which is larger than $\omega_e\sigma_z/c$ is mean less. To remove the ambiguity, we have to do tracking simulations [2–4].

We show simulation results using a strong-strong code, named PEHTS [4]. A bunch and electron cloud are expressed by macro-particles, the interaction between them are calculated by solving two dimensional Poisson equation with the particle in cell method.

The interaction between beam and cloud is evaluated at several or several tens position in a ring, where beta function is uniform. Since the interaction is discrete, an artificial incoherent emittance growth sometimes appears. The head-tail instability has to be distinguished from the artificial incoherent effect. Head-tail effect can be simulated by a sufficient number of interactions in a synchrotron period, therefore it does not depend on the number of interaction in a revolution. To get the threshold of the fast head-tail instability, the emittance growth is checked whether independent of the number of interaction. Beam-cloud profile is also monitored to distinguish the incoherent effect. If the fast head-tail instability occurs in the simulation, bunch and cloud centroid move along the bunch length coherently.

We do not deny the exist of all of the incoherent effect. Increasing the number of interaction with uniform beta function does not give true incoherent emittance growth. The incoherent effect is treated in next section.

Figure 1 shows emittance growth due to the fast head-tail instability caused by electron cloud for the damping ring lattices. Each plot shows an emittance growth for various cloud densities. The threshold density is determined by the density in which the growth start.

Figure 2 shows the snapshot of the beam and cloud amplitude and beam size along the bunch length above the threshold. Amplitude of beam-cloud coherent motion is similar as beam size increase. We can say the fast head-tail instability is dominant.

The threshold values are summarized in Table III. The analytical estimates are compared with those given by simulation. The density given by the simulation is systematically lower than them. We suppose that the lower threshold density in the simulation is caused by pile up and pinching of electrons due to the attractive force of beam. The characteristics constant of the attractive force is the electron phase advance in the beam, $\omega_e\sigma_z/c$: i.e. a higher phase advance lowers the threshold density. In B factories, the phase advance is far lower than damping rings, therefore the analytical estimate coincides with the simulation. We should use the threshold value given by the simulation for the estimation of the instability.

Table III: Threshold density for fast head-tail type of electron cloud instability in damping rings.

Lattice	TESLA	TESLA*	MCH	DAS	OCS	BRU	OTW	PPA	KEKB	PEP-II
$\rho_{e,th}(10^{12} \text{ m}^{-3})$	0.54	1.29	1.34	0.47	0.62	2.28	1.70	1.31	0.53	
$\rho_{e,sim}(10^{12} \text{ m}^{-3})$	0.12	0.24	0.30	0.12	0.14	0.3	0.4	-	0.4	-
$\omega_e\sigma_z/c$	14.5	17.3	15.9	13.3	12.6	17.5	14.7	15.4	3.1	
$\Delta nu_y(\rho_{e,sim})$	0.018	0.018	0.041	0.018	0.0074	0.021	0.011		0.005	

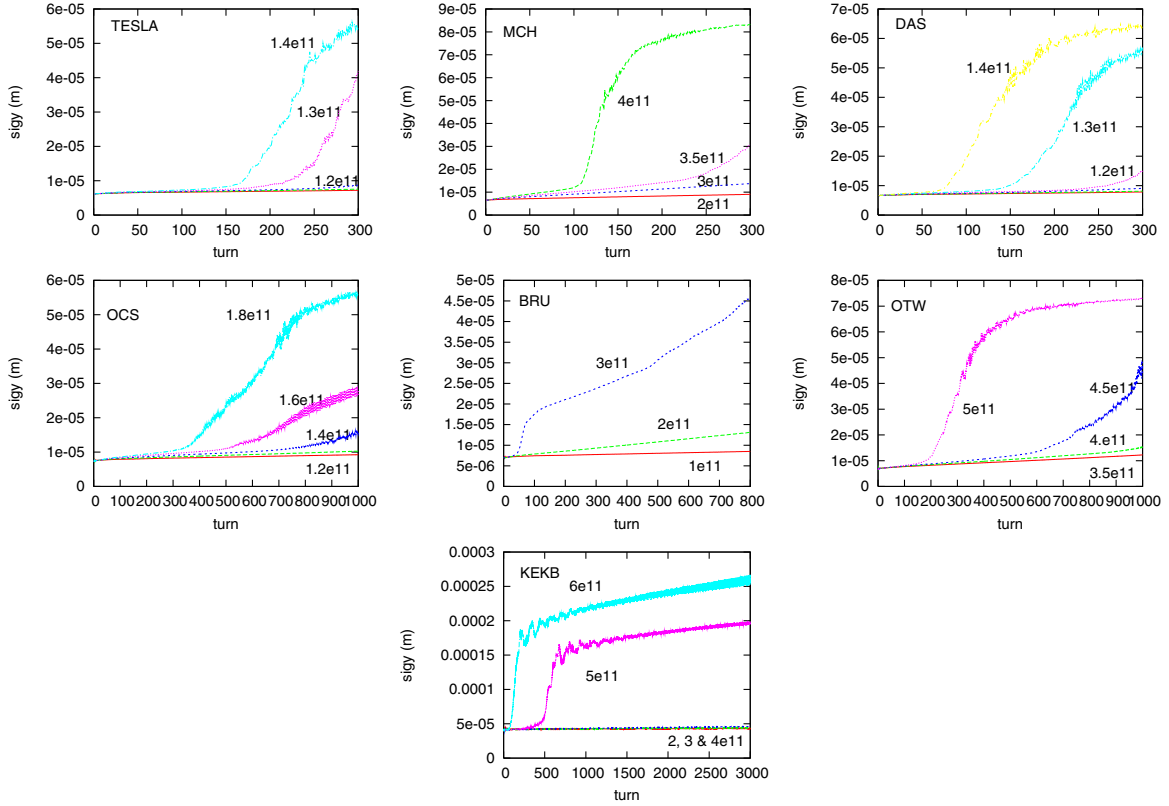


Figure 1: Emittance growth due to the fast head-tail instability caused by electron cloud.

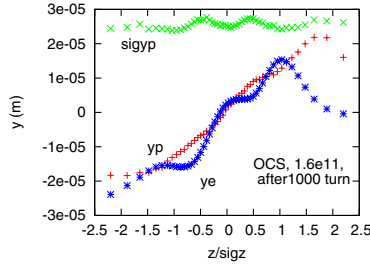


Figure 2: Beam and cloud profile along the bunch length. Bunch size and centroid of bunch and cloud along the bunch length are plotted.

3. INCOHERENT EMITTANCE GROWTH

The tune shift near the threshold density of the instability is not very large as shown in Table III. However electrons are raked and pinched by the beam force, with the result that the density near the beam and tune shift increases with the process of the interaction along the longitudinal (bunch length). The cloud densities before beam interaction and at the interaction with bunch center ($z = 0$) are depicted in Figure 3. The density increases 30 times higher at a narrow area of the beam center in the picture (a) to (b), therefore tune shift increases to more than 0.5 at the threshold value.

This type of emittance growth is caused by a symplectic diffusion due to nonlinear force [5, 6]. In a periodic system like a circular accelerator, the nonlinearity of the whole ring is characterized by one turn map. The one turn map is expressed by

$$M = e^{-:F_{1,n}:} e^{-:\phi_n:} \dots e^{-:F_{3,2}:} e^{-:\phi_2:} e^{-:F_{2,1}:} e^{-:\phi_1:} \quad (5)$$

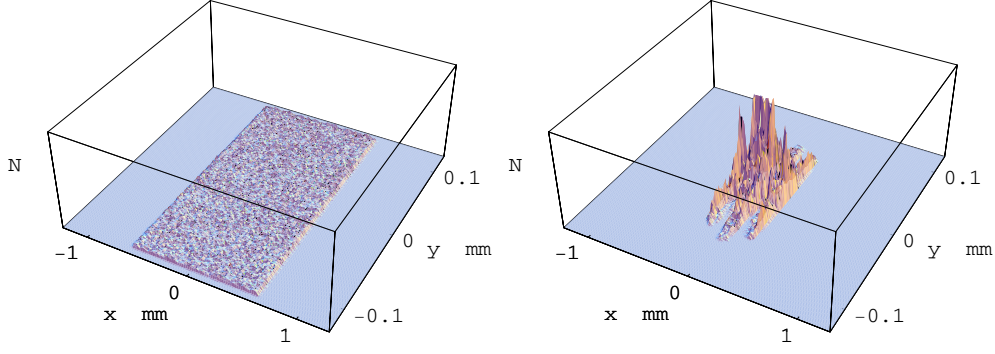


Figure 3: Electron cloud density (a) before interaction with a bunch, (b) at the interaction with bunch center ($z = 0$).

where $e^{-:F_{i,i-1}:}$ is the transfer map due to lattice elements between s_{i-1} to s_i , and ϕ is electric potential of electron cloud. Nonlinearity of the map

$$e^{-:F_1:} \prod_i e^{:F_{i,1}:} e^{-:\phi_i:} e^{-:F_{i,1}:} = e^{-:F_1:} T \exp \left\{ - \int : \phi(e^{-:F_{i,1}:} \mathbf{x}) : ds_i \right\} \quad (6)$$

where $e^{-:F_{i,1}:}$ is the transfer map from s_1 to s_i . The integral is performed with considering the beta function and betatron phase at the cloud position s_i .

We integrate motion of beam particles along the lattice element by element. Since the integration is very time consuming, we use a simplified model. In many rings, cell structure with a certain betatron phase advance is used. We take a series of cell with the betatron phase advance of $2m\pi$.

$$M(2m\pi) = e^{-:F_{c,2m\pi}:} T \exp \left\{ - : \phi(e^{-:F_{i,c}:} \mathbf{x}) : \right\} \quad (7)$$

where $e^{-:F_{c,2m\pi}:}$ is the linear map with $2m\pi$ phase advance, that is, it is identity map. If the whole ring consists of N cell and the electron potential (ϕ) is periodic for the cell, one turn map can be modeled as

$$M = e^{-:F_{fr}:} \frac{N}{m} T \exp \left\{ - \int_{\text{cell}} \phi(e^{-:F_{i,c}:} \mathbf{x}) : ds_i \right\} \quad (8)$$

where $e^{-:F_{fr}:}$ is the linear map to adjust fractional tune. Furthermore ϕ is symmetric for $x \rightarrow -x$ and/or $y \rightarrow -y$, it is enough to take into account of $m\pi$ cell not $2m\pi$. Using this model, computation time can be saved drastically.

In dogbone type of damping ring, electrons, which are build up in the wiggler section, are considered to give a dominant contribution for the instability. The wiggler section is consist of 60 degree FODO cell. The phase advance is π and 2π for 3 and 6 cell, respectively. We compare the emittance growth for 3 and 6 cell model. Integrated density is kept for both cases. Figure 4 shows the lattice of the wiggler section and emittance growth for 3 cell (π phase advance) and 6 cell (2π) for three different cloud densities. Two lines for 3 and 6 cell at each density coincide well.

Figure 5 shows emittance growth for various cloud density. We have emittance growth at the density of $\rho_e = 10^{12} \text{ m}^{-3}$ for TESLA. The threshold is higher than that given by uniform beta model. Now tracking time is limited 300 turns. It may be too short to get head-tail instability. In MCH, the threshold, which is $\rho_e = 4 \times 10^{11} \text{ m}^{-3}$, is consistent with that by the uniform beta model. Figure 6 shows bunch and cloud profiles for TESLA and MCH. In both case, clear coherent motion can not be seen, though emittance growth is seen. Coherent motion may be smeared by the strong nonlinear force. It is safe to use the threshold value given by the uniform beta model.

We next discuss OCS lattice, whose twiss parameter is shown in Figure 7. Phase advance of the cell is 3π and 2π for the horizontal and vertical planes, respectively. Figure 8 shows the emittance growth for this OCS model. Plots (a) and (b) depict the emittance growth in the case that electrons filled whole of cell and filled only in bending

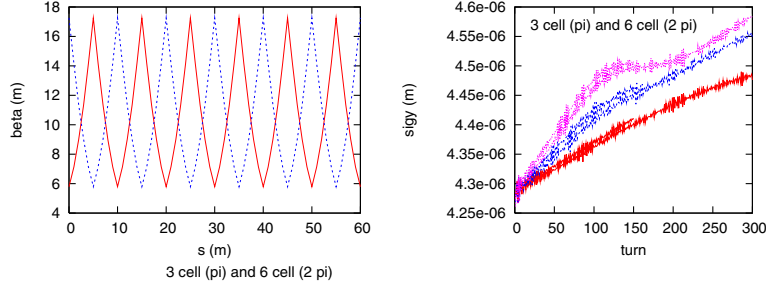


Figure 4: (a) Structure of the wiggler cell. (b) Comparison of π and 2π for 3 and 6 cell.

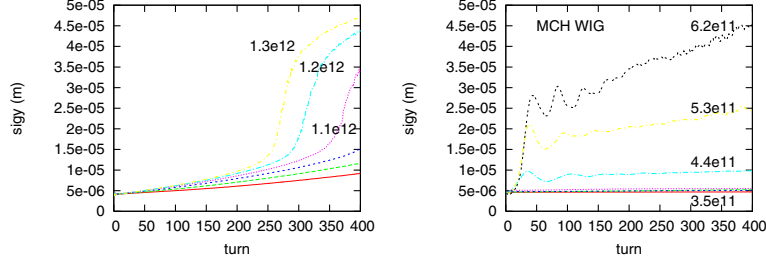


Figure 5: Emittance growth caused by electron cloud for TESLA and MCH. Electron cloud only in wiggler magnet is considered.

magnets, respectively. The threshold is given as $\rho_{e,av} = 7.7 \times 10^{11} \text{ m}^{-3}$, which is a half of that of uniform beta model, see Figure 1 and Table III. Plot (c) depicts a slower emittance growth at the cloud densities lower than the threshold. We understand that this growth is due to the incoherent effect. The growth rate, which is $0.5 \times 10^{-3} \sigma_y/\text{turn}$, is less than radiation damping rate 2×10^{-3} , and the growth is saturated at 10% increase, therefore it does not seem to be serious. This fact means that the coherent fast head-tail instability dominates for the incoherent growth in OCS.

We have to notice the lower threshold than that for the uniform beta model. Since the dispersion is not taken into account in the uniform beta model, the horizontal beam size is different from that of this real lattice model. Contributions to the horizontal beam size of the dispersion is dominant: i.e., $\varepsilon_x \beta_x = 5.3 \times 10^{-9} \text{ m}^2$ and $(\eta \sigma_\delta)^2 = 6.7 \times 10^{-8} \text{ m}^2$. To check an effect of the dispersion, we compare this result with two cases without dispersion, in which emittance is kept but beam size is 1/3.3, and the beam size is kept but emittance is 10 times higher. Figure 10 shows the emittance growth for these two cases. In either case, the threshold, which is $1.2 - 1.4 \times 10^{11} \text{ m}^{-3}$, is consistent with that given by uniform beta model. The dispersion in the arc section worsens the instability.

4. COUPLED BUNCH INSTABILITY

The coupled bunch instability is caused by a long range ($\sim \text{m}$) wake field induced by the electron cloud. The feature of the wake field strongly depends on electron motion in the cloud. The wake in drift space has a low quality factor ($Q \sim 1$), while that in magnetic field tends to have a higher Q . R/Q is determined by the number of electrons which contributes the instability. We discuss the coupled bunch instability due to electrons in drift space here. Actual instability is determined by summation of the wake field of every sections of drift, bending, quadrupole and wiggler.

Figure 11 shows the wake field for OCS and OTW rings. The cloud line density is $\lambda_e = 5 \times 10^7$ and $7 \times 10^7 \text{ m}^{-1}$, respectively, in this calculation.

The growth rate of the coupled bunch instability is estimated by the formula [7]

$$(\Omega_m - \omega_\beta)L/c = \frac{N_+ r_e c}{2\gamma\omega_\beta} \sum_{k=1}^n W_1(-kL_{sp}) e^{2\pi i k(m+\nu_\beta)/M}, \quad (9)$$

Figure 12 shows the growth of the coupled bunch mode caused by electron cloud.

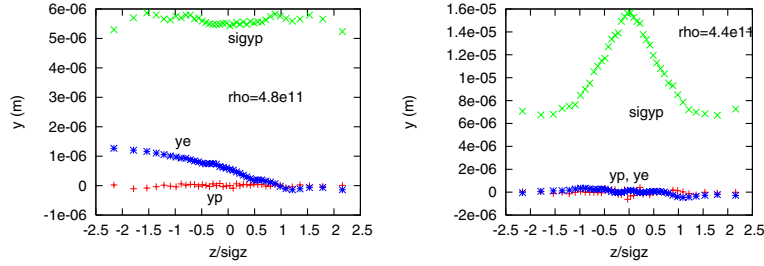


Figure 6: Beam and cloud profile above the threshold for TESLA and MCH.

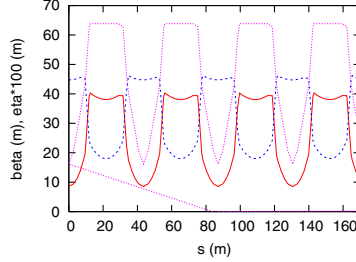


Figure 7: OCS lattice. Phase advance of the cell is 3π and 2π for horizontal and vertical planes, respectively.

The growth rate was obtained as $10\mu\text{s}$ (500 turn) and $7.5\mu\text{s}$ (700 turn) for OCS and OTW rings, respectively. It is possible to be cured for the growth by using a bunch-by-bunch feedback system.

The growth rate is estimated for whole ring covered by various kinds of magnets [8] in next step.

5. CONCLUSION

We evaluated electron cloud instabilities in the candidates of the ILC damping ring.

Threshold of the fast head-tail instability was estimated by analytic theory and a strong-strong type of simulation using uniform beta model. The threshold cloud density is summarized in Table III. The threshold values given by the simulation are a factor 4-5 less than those by analytic formula. The difference is caused by pile up and pinching of electrons due to the beam force. We use the value given by the simulation for the damping ring design.

The electron cloud, especially pile up and pinched by the beam, induces tune shift of the beam. The tune shift can cause incoherent emittance growth. To study the incoherent emittance growth, the motion of the beam particle should be integrated with interaction with electron cloud along the real lattice. Incoherent effect have been studied using a simplified lattice model. The growth (diffusion) rate is not serious for OCS. Coherent fast head-tail instability dominates in OCS and it is made worse by the dispersion function of lattice. In TESLA and MCH with a large circumference, any clear signal of the coherent fast head-tail instability was not seen even higher cloud density than that determine by the uniform beta model. Though incoherent effect seems to dominate in the large rings, the emittance growth was not serious.

The coupled bunch instability is evaluated for electrons in drift space. That for various magnet will be evaluated soon.

The author thanks X. Dong, Y. Ohnishi, M. Pivi, A. Wolski, R. Wanzenberg and F. Zimmermann for fruitful discussions.

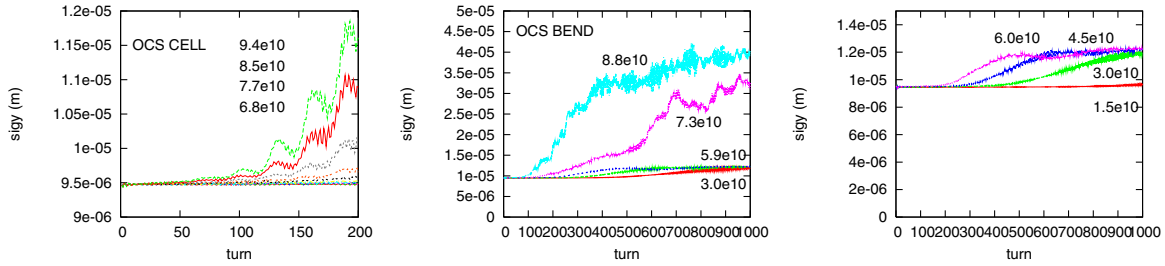


Figure 8: Emittance growth caused by electron cloud for OCS, in which (a) electrons are filled in the whole lattice, (b) electrons are localized in the bending magnet and (c) slow emittance growth below the threshold.

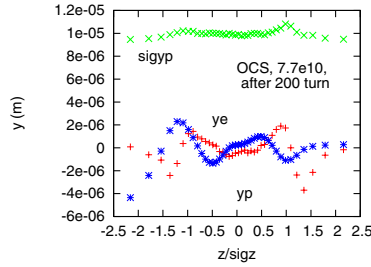


Figure 9: Beam and cloud profile above the threshold for OCS.

References

- [1] K. Ohmi, F. Zimmermann, E. Perevedentsev, Phys. Rev. E **65**, 16502 (2002).
- [2] K. Ohmi and F. Zimmermann, Phys. Rev. Lett., **85**, 3821 (2000).
- [3] G. Rumolo et. al., Proceedings of PAC2001, 1889 (2001).
- [4] K. Ohmi, Proceedings of PAC2001, 1895 (2001).
- [5] K. Ohmi et. al., Phys. Rev. ST-AB, **7**, 104401 (2004).
- [6] E. Benedetto et al., Proceedings of PAC2005.
- [7] A.W. Chao, *Physics of Collective Beam Instabilities in High Energy Accelerators*, Wiley-Interscience Publication.
- [8] S. Win et al., Phys. Rev. ST-AB, **8**, 094401 (2005).

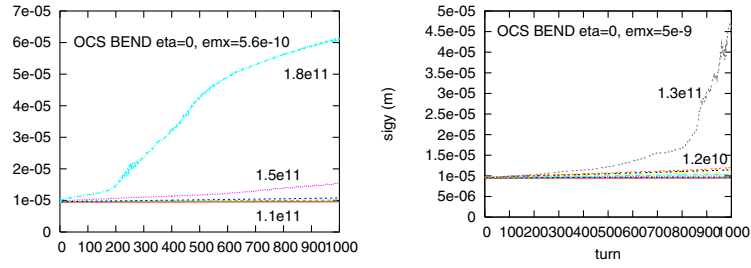


Figure 10: Emittance growth caused by electron cloud for OCS. Parameters are chosen as (a) $\varepsilon_x = 0.56 \times 10^{-9}$ m (nominal) and $\eta = 0$, and (b) $\varepsilon_x = 0.56 \times 10^{-8}$ m, $\sigma_x =$ and $\eta = 0$.

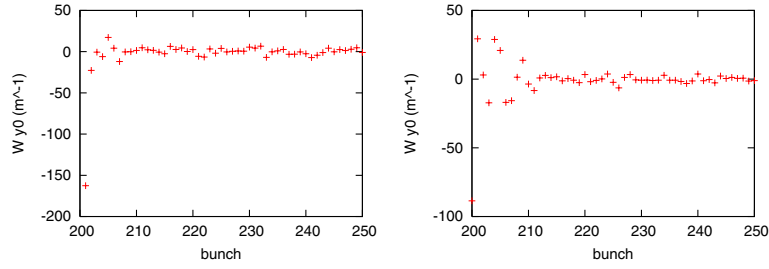


Figure 11: Long range wake field induced by the electron cloud in (a) OCS (b) OTW.

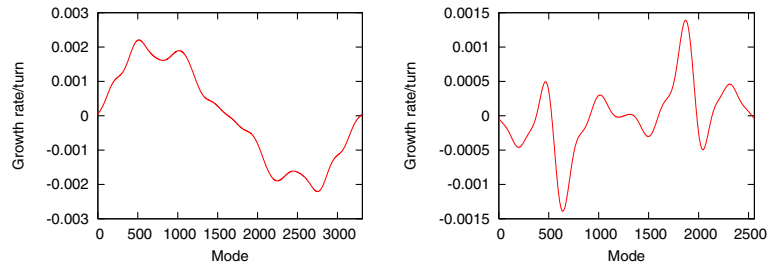


Figure 12: Growth rate for coupled bunch instability caused by the electron cloud in (a) OCS (b) OTW.